

Raman Scattering by Carriers in Landau Levels

Y. YAFET

Bell Telephone Laboratories, Murray Hill, New Jersey

(Received 26 July 1966)

The cross sections for Raman scattering by electrons and holes in a semiconductor subjected to a magnetic field are calculated. A number of processes in which the Landau level number changes by $\Delta n=2$, as well as a spin-flip process with $\Delta n=0$, are considered. Except for the $\Delta n=2$ process in the conduction band, the matrix elements are independent of the strength of the magnetic field. Scattering cross sections are estimated for InSb (incident photon energy 0.12 eV) and InP (incident photon energy 1.17 eV). The magnitude of these cross sections suggests that it may be possible to use Raman scattering to measure effective masses.

I. INTRODUCTION

THE scattering of light by mobile carriers in a crystal has recently been considered by Wolff.¹ Of particular interest to us here is a Raman process in the presence of a magnetic field: An electron, initially in the Landau level n , scatters a photon and makes a transition to the level $n+2$ the frequency of the photon being shifted by twice the cyclotron frequency. Wolff confined his considerations to a nondegenerate band, and he made use of a simple two-band model to estimate the cross section for this process.

In this paper we extend his calculation in two ways: (1) the actual band structure and wave functions of indium-antimonide-type crystals are used to calculate the cross section for carriers in the conduction band, and (2) other Raman processes are considered, specifically (a) hole scattering in the degenerate valence band, and (b) spin reversal transitions in the conduction and valence bands.

As was expected, for the process calculated by Wolff our answer is very similar to his. However for the other processes we find a different dependence of the matrix element on the magnetic field, i.e.: For the transition among valence-band states the lowest order matrix element is independent of field-strength and photon energy; for spin-reversal transitions in the conduction band, it is independent of field-strength and proportional to the photon energy. In InSb all types of matrix elements are comparable at fields of a few kG and at still higher fields the $\Delta n=2$ process in the conduction band is favored. However in larger band gap materials such as InP, the $\Delta n=1$ and $\Delta n=2$ transitions in the valence band have the larger cross sections. With a laser source it is expected that these Raman processes will be observed and that they may give information on the band structure.

II. CALCULATION OF THE MATRIX ELEMENTS

We use a simplified model for the conduction and valence bands in the neighborhood of $k=0$, i.e., we neglect the interaction with other bands and also the free mass terms. This is known to be an excellent

approximation in many cases, and it makes it possible to obtain the wavefunctions in the presence of a magnetic field² and hence to calculate the matrix elements. The neglected bands may change the values of numerical coefficients in the matrix elements, but not the form of their dependence on the energies of interest (i.e., photon, cyclotron, and band gap energies.)

The expansion coefficients for the wave functions are shown on Table 1. Here S, X, Y, Z are, respectively, the conduction and valence band states in the absence of spin-orbit coupling at the center of the zone; $P = \langle iS | p_x | X \rangle$ is the momentum matrix element, Δ the spin-orbit splitting, the magnetic field is in the z direction, $s = eH/\hbar c$, and Φ_n is the n 'th harmonic oscillator function of the variable k_x/\sqrt{s} . The $\lambda_{n\sigma}^{(\alpha)}$, for $\alpha = c, l, s$, are the energies of the one-electron eigenstates (with the magnetic field) of the conduction band, the light-hole band, or the split-off band, respectively. They are obtained from Eq. (5) in Ref. 2, and it will be convenient to have their expression to order k^2 , which is given by (taking $\hbar = m = 1$):

$$\lambda_{n\sigma}^{(\alpha)} = E^{(\alpha)} + \frac{1}{2m_\alpha} [k_z^2 + s(2n+1)] + \frac{\sigma}{2m_{\alpha'}} s$$

where m_α and $m_{\alpha'}$ are the orbital and spin masses, respectively, and $\sigma = \pm 1$ corresponds to \uparrow and \downarrow spin. For the conduction band, $\alpha = c$:

$$E^{(c)} = E_G; \quad \frac{1}{2m_c} = \frac{1}{3} \left(2 \frac{P^2}{E_G} + \frac{P^2}{E_G + \Delta} \right);$$

$$\frac{1}{2m_{c'}} = -\frac{1}{3} \left(\frac{P^2}{E_G} - \frac{P^2}{E_G + \Delta} \right).$$

For the light hole band, $\alpha = l$:

$$E^{(l)} = 0; \quad \frac{1}{2m_l} = -\frac{2}{3} \frac{P^2}{E_G}; \quad \frac{1}{2m_{l'}} = \frac{1}{3} \frac{P^2}{E_G}.$$

² R. Bowers and Y. Yafet, Phys. Rev. **115**, 1165 (1959); Y. Yafet, *ibid.* **115**, 1172 (1959). As explained in this paper, as long as the energy bands of interest can be approximated by spherical bands, their magnetic levels can be obtained exactly.

¹ P. A. Wolff, Phys. Rev. Letters **16**, 225 (1966).

TABLE I. Wave functions in a magnetic field: The Φ_n are functions of k_x (k representation). Atomic units $\hbar=m=1$ are used, and the other symbols are defined in the text. $|\text{hh},n\sigma\rangle$ denote the two ($\sigma=\uparrow$ and \downarrow) heavy hole states; $|\alpha,n\sigma\rangle$ denotes either one of a conduction, light hole, or split-off band state. The wave functions in these last three bands have a formal similarity and are differentiated only by the values of the energy $\lambda_{n\sigma}^{(\alpha)}$. The normalization of the states gives a further common factor which is not included in the table. The values of n are: $n \geq 0$ for $|\alpha,n\sigma\rangle$; $n \geq -1$ for $|\text{hh},n\downarrow\rangle$; $n \geq +1$ for $|\text{hh},n\uparrow\rangle$.

Basis states	$ \alpha,n\downarrow\rangle$	$ \alpha,n\uparrow\rangle$	$ \text{hh},n\downarrow\rangle$	$ \text{hh},n\uparrow\rangle$
$iS\downarrow$	Φ_n			
$iS\uparrow$		Φ_n		
$\frac{1}{\sqrt{2}}(X-iY)\downarrow$	$\frac{P}{\lambda_{n\downarrow}^{(\alpha)}}\{s(n+1)\}^{1/2}\Phi_{n+1}$		Φ_{n+1}	
$(\sqrt{\frac{3}{2}})Z\downarrow + \sqrt{\frac{1}{6}}(X-iY)\uparrow$	$(\sqrt{\frac{3}{2}})\frac{P}{\lambda_{n\downarrow}^{(\alpha)}}k_z\Phi_n$	$(\sqrt{\frac{3}{2}})\frac{P}{\lambda_{n\uparrow}^{(\alpha)}}\{s(n+1)\}^{1/2}\Phi_{n+1}$	$-\frac{(\sqrt{6})k_z\{s(n+1)\}^{1/2}}{2k_z^2+sn}\Phi_n$	$-\frac{\sqrt{3}s\{n(n+1)\}^{1/2}}{2k_z^2+s(n+1)}\Phi_{n+1}$
$(\sqrt{\frac{3}{2}})Z\uparrow - \sqrt{\frac{1}{6}}(X+iY)\downarrow$	$-(\sqrt{\frac{3}{2}})\frac{P}{\lambda_{n\downarrow}^{(\alpha)}}(sn)^{1/2}\Phi_{n-1}$	$(\sqrt{\frac{3}{2}})\frac{P}{\lambda_{n\uparrow}^{(\alpha)}}k_z\Phi_n$	$\frac{\sqrt{3}s\{n(n+1)\}^{1/2}}{2k_z^2+sn}\Phi_{n-1}$	$-\frac{(\sqrt{6})k_z(sn)^{1/2}}{2k_z^2+s(n+1)}\Phi_n$
$\frac{1}{\sqrt{2}}(X+iY)\uparrow$		$\frac{P}{\lambda_{n\uparrow}^{(\alpha)}}(sn)^{1/2}\Phi_{n-1}$		Φ_{n-1}
$(\sqrt{\frac{3}{2}})Z\downarrow - \sqrt{\frac{1}{6}}(X-iY)\uparrow$	$(\sqrt{\frac{3}{2}})\frac{P}{\lambda_{n\downarrow}^{(\alpha)}+\Delta}k_z\Phi_n$	$-(\sqrt{\frac{3}{2}})\frac{P}{\lambda_{n\uparrow}^{(\alpha)}+\Delta}\{s(n+1)\}^{1/2}\Phi_{n+1}$		
$(\sqrt{\frac{3}{2}})Z\uparrow + \sqrt{\frac{1}{6}}(X+iY)\downarrow$	$(\sqrt{\frac{3}{2}})\frac{P}{\lambda_{n\downarrow}^{(\alpha)}+\Delta}(sn)^{1/2}\Phi_{n-1}$	$(\sqrt{\frac{3}{2}})\frac{P}{\lambda_{n\uparrow}^{(\alpha)}+\Delta}k_z\Phi_n$		

For the split-off band, $\alpha=s$,

$$E^{(s)} = -\Delta; \quad \frac{1}{2m_s} = -\frac{1}{3} \frac{P^2}{E_G + \Delta}; \quad \frac{1}{2m_{s'}} = -\frac{1}{3} \frac{P^2}{E_G + \Delta}.$$

The heavy holes have infinite mass in this approximation.

Of the two terms in $\mathbf{p} \cdot \mathbf{A}$ and A^2 of the electron-photon interaction, the A^2 term does not contribute to Raman scattering in the dipole approximation³ and the matrix element is due to $\mathbf{p} \cdot \mathbf{A}$ taken in second order. Written fully, this term is

$$\mathcal{C}' = G \sum_{q,\lambda} \frac{1}{(m\omega_q)^{1/2}} (\mathbf{e}_{q\lambda} \cdot \mathbf{p} e^{iq \cdot \mathbf{r}} a_{q\lambda} + \mathbf{e}_{q\lambda}^* \cdot \mathbf{p} e^{-iq \cdot \mathbf{r}} a_{q\lambda}^+),$$

where $a_{q\lambda}$ and $a_{q\lambda}^+$ are the destruction and creation operators for photons of polarization $\mathbf{e}_{q\lambda}$ and frequency ω_q . The constant G is given by

$$G = \left(\frac{e^2}{mc^2} \right)^{1/2} \left(\frac{2\pi\hbar c^2}{\epsilon V} \right)^{1/2},$$

where m is the free electron mass and ϵ the dielectric constant and V the volume of the sample. The matrix element for the absorption of a photon (q_0, ω_0) and emis-

sion of a photon (q_1, ω_1) with polarizations \mathbf{e}_0 and \mathbf{e}_1 is

$$(\mathcal{C}')_{f_0} = G^2 \frac{1}{(\omega_0 \omega_1)^{1/2}} A_{f_0},$$

where the dimensionless quantity A_{f_0} is

$$A_{f_0} = \frac{1}{m} \sum_r \left(\frac{(\mathbf{e}_1^* \cdot \mathbf{p})_{fr} (\mathbf{e}_0 \cdot \mathbf{p})_{r0}}{E_0 + \hbar\omega_0 - E_r} + \frac{(\mathbf{e}_0 \cdot \mathbf{p})_{fr} (\mathbf{e}_1^* \cdot \mathbf{p})_{r0}}{E_0 - \hbar\omega_f - E_r} \right). \quad (1)$$

Here o , r , and f refer to the initial, intermediate and final states of the electron, and E_0 , E_r and E_f are the corresponding energies. By energy conservation $E_0 + \hbar\omega_0 = E_f + \hbar\omega_1$. The differential scattering cross section is given by

$$\left(\frac{d\sigma}{d\Omega} \right)_{f_0} = \left(\frac{e^2}{mc^2} \right) \frac{\omega_1}{\omega_0} |A_{f_0}|^2.$$

The dielectric constant has cancelled out and the effect of the band structure is contained entirely in the quantity A_{f_0} which is to be calculated with the eigenstates of Table I. Because the energy values $\lambda_{n\sigma}^{(\alpha)}$ are complicated functions of ns and k_z^2 , an exact calculation with these states would involve considerable computational work. We shall be content with an approximate A_{f_0} and, hence, we expand $\lambda_{n\sigma}^{(\alpha)}$ and the coefficients in Table I in powers of s and k_z^2 . To obtain A_{f_0} to order H (or s) we include in the expansion of these coefficients terms of order $s^{3/2}$. The calculations are straightforward but tedious and only the results are given below.

³ The dipole approximation will be valid as long as $qr \ll 1$, q being the photon wave vector in the solid and r the cyclotron radius. For the lowest level, $n=0$, this requires $H \gg 400E^2\epsilon$ where E is the photon energy in eV and ϵ is the dielectric constant.

To abbreviate the writing, the eigenstates of the conduction band, the light hole band, and the heavy hole band have been denoted by $|c,n\sigma\rangle$, $|lh,n\sigma\rangle$, and $|hh,n\sigma\rangle$, respectively.

Conduction Band

(a) Orbital transitions

The matrix element for the $|c,n\sigma\rangle$ to $|c,n+2\sigma\rangle$ transition is the same for \uparrow and \downarrow spin and is given by

$$A_{f0} = 2\{(n+1)(n+2)\}^{1/2} \frac{m \hbar \omega_c (2E_G + 2\Delta)^2}{m_c E_G (3E_G + 2\Delta)} \times \left\{ \frac{E_G^2}{E_G^2 - (\hbar\bar{\omega}_0)^2} \left(1 + \frac{3E_G}{8\Delta} + \frac{E_G}{8E_G + \Delta} \right) + \frac{3\Gamma}{8} \frac{E_G \hbar\bar{\omega}_0}{E_G^2 - (\hbar\bar{\omega}_0)^2} \right\}^2 + \frac{1}{8} \frac{E_G^2}{(E_G + \Delta)^2 - (\hbar\bar{\omega}_0)^2} \left(1 + \frac{2E_G}{E_G + \Delta} - \frac{3E_G}{\Delta} \right) \left(\frac{\epsilon_{0x} - i\epsilon_{0y}}{\sqrt{2}} \right) \left(\frac{\epsilon_{1x} + i\epsilon_{1y}}{\sqrt{2}} \right) \dots, \quad (2)$$

where $\bar{\omega}_0 = \frac{1}{2}(\omega_0 + \omega_1)$. The circular polarization of the incident photon is the same as for cyclotron resonance (i.e., counterclockwise around the field direction) while the out-going photon has the *opposite* sense of polarization.

In Eq. (2) we have neglected terms of order ω_c/ω_0 and $\hbar^2 k_z^2/m_c E_G$. The first two terms in the curly bracket are contributed by the upper valence band and the last term by the split-off band. In the limit $\omega_0 \rightarrow 0$ and both for $\Delta=0$ and $\Delta=\infty$ Eq. (2) reduces to the expression of the two-band model of Ref. 1. The second term (which varies as $(E_G^2 - \hbar\bar{\omega}_0^2)^{-2}$) is specific to a degenerate valence band and it gives a further enhancement of the cross-section for values of $\hbar\bar{\omega}_0$ very close to E_G .

In calculating A_{f0} it is found that the light hole intermediate state contributes in order $P^2/mE_G \sim m/m_c$. The heavy hole intermediate state contributes in the same order but the two cancel each other exactly in lowest order and the net result is of order $(m/m_c)(\hbar\omega_c/E_G)$. This raises the question whether the cancellation is an artificial feature of the simple model used here. The answer is that for carriers in a nondegenerate band the cancellation will always occur, and one way to see this is as follows: If A_{f0} were really of order m/m_c

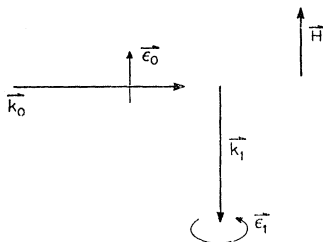


FIG. 1. Possible geometry for observing spin-reversal transitions.

and hence independent of the magnetic field, then by the principle of spectroscopic stability it should be unnecessary to use the exact states of the valence band in calculating it, since the splittings in the valence band are of order $\hbar\omega_c$. If we take valence states which are a single product of a cell-periodic function and a harmonic oscillator function, it becomes obvious by inspection that there are no Raman matrix elements of order m/m_c . In Figs. 2 and 3 we have plotted the dimensionless quantity h_{f0} (which is A_{f0} without the polarization factors) for $n=0$ and $k_z=0$ as a function of magnetic field, for InSb and InP, respectively. For the former, the photon energy of a CO₂ laser (0.12 eV) was taken. InP was chosen as a second example because its band gap of 1.34 eV is only slightly larger than the 1.17 eV photon of a neodymium laser, thus providing a large enhancement factor $(E_G^2 - \hbar\omega_0^2)^{-1}$.

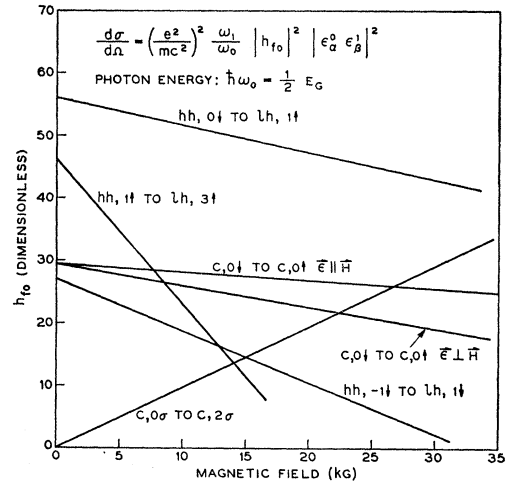


FIG. 2. Matrix elements for Raman scattering in InSb.

At a given field, h_{f0} is about 20 times smaller in InP than in InSb. This is because $h_{f0} \sim (m/m_c)(\hbar\omega_c/E_G) \sim (P^4/E_G^3)$ is inversely proportional to the cube of E_G , which would result in a ratio of 200, but this ratio is reduced to 20 by the enhancement factor being much larger in InP than in InSb.

(b) Spin Reversal Transitions

The simple product states $u_{3/2, m_j} \Phi_n$ of the last paragraph make it easy to see that the matrix element for spin reversal remains finite for a vanishing magnetic field. Thus if the incident photon is polarized along the z direction, the outgoing photon will be circularly polarized and for the $|c,n\uparrow\rangle$ to $|c,n\downarrow\rangle$ transition, the intermediate state $u_{3/2, 1/2} \Phi_n$ will contribute to the first term of (1) while $u_{3/2, -1/2} \Phi_n$ will contribute to the second term. If the g factor is negative as in InSb, then $\lambda_{n\downarrow}^{(e)} > \lambda_{n\uparrow}^{(e)}$ and the outgoing photon will be polarized counterclockwise; the sense of polarization will be

opposite if the g factor is positive, as is probably the case in InP. (Actually the g factor of InP is expected to be of the order of 0.8, which would give a very small Raman shift and make resolution difficult.) A possible geometry for observing this Raman effect is shown in Fig. 1.

The complete matrix element is obtained by including the split-off band, and the result to lowest order in H for the $|c,n\uparrow\rangle$ to $|c,n\downarrow\rangle$ transition is

$$A_{f0} = \frac{2\sqrt{2} P^2 \hbar \omega_0}{3 m E_G^2} \left[\frac{E_G^2}{E_G^2 - (\hbar \omega_0)^2} - \frac{E_G^2}{(E_G + \Delta)^2 - (\hbar \omega_0)^2} \right] \times \left[\frac{(\epsilon_{1x} - i\epsilon_{1y})}{\sqrt{2}} \frac{(\epsilon_{0x} + i\epsilon_{0y})}{\sqrt{2}} \epsilon_{1z} \right]. \quad (3)$$

The dependence of A_{f0} on $\hbar \omega_0$ is the same as for the

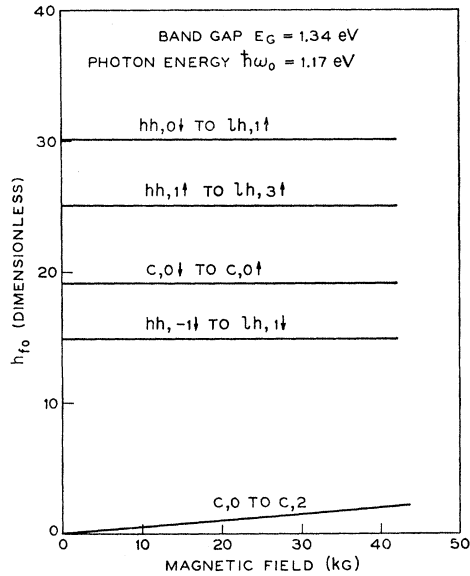


FIG. 3. Matrix elements for Raman scattering in InP.

Raman scattering of phonons⁴ in spin-lattice relaxation. Notice that even if Δ is small (as in InP) the second term of the first bracket is small relative to the first if $\hbar \omega_0$ is very close to E_G .

The magnitude of A_{f0} is plotted in Figs. 2 and 3, and it is seen that unlike the A_{f0} of the $\Delta n = 2$ transition, it is comparable for InSb and InP. The reason for the difference is that for an $\hbar \omega_0$ comparable to E_G , A_{f0} in (3) is inversely proportional to only the first power of E_G .

There is also another allowed transition involving a spin flip, i.e., $|c,n\uparrow\rangle$ to $|c,n+2\downarrow\rangle$. The magnitude of h_{f0} for this transition is however only of order $(\hbar \omega_c/E_G)$ (P^2/mE_G); the polarization factors are $\epsilon_{0z}(\epsilon_{1x} + i\epsilon_{1y})$ and $(\epsilon_{0x} - i\epsilon_{0y})\epsilon_{1z}$. The Raman shift of $2\hbar \omega_c + 2(m/m_c')\beta H$ would be the largest in the conduction band.

⁴ See, e.g., R. Orbach, Proc. Phys. Soc. (London) **77**, 821 (1961).

TABLE II. Transitions in the valence band. Values of the factor N_{f0} of Eq. (4) for the matrix element.

Initial state	Final state	n	N_{f0}
$hh,n\downarrow$	$lh,n+2\downarrow$	$n \geq -1$	$\frac{2}{3} \left\{ \frac{3n(n+2)}{(4n+3)(4n+11)} \right\}^{1/2}$
$hh,0\downarrow$	$lh,1\uparrow$	$n = 0$	$\frac{2}{\sqrt{5}}$
$hh,n\uparrow$	$lh,n+2\uparrow$	$n \geq 1$	$2 \left\{ \frac{3n(n+2)}{(4n+1)(4n+9)} \right\}^{1/2}$
$lh,n\downarrow$	$lh,n+2\downarrow$	$n \geq 0$	$2 \left\{ \frac{(n+1)(n+2)}{(4n+3)(4n+11)} \right\}^{1/2}$
$lh,n\uparrow$	$lh,n+2\uparrow$	$n \geq 0$	$2 \left\{ \frac{(n+1)(n+2)}{(4n+1)(4n+9)} \right\}^{1/2}$

Valence Band

(a) $\Delta n = 2$

The near cancellation between contributions from the light holes and the heavy holes, which gave $A_{f0} \sim \hbar \omega_c$ for the conduction band, does not come into play for transitions in the valence band, and A_{f0} becomes of order P^2/mE_G . This result can be easily checked from the wave functions of Table I, as any valence band state (at $k_x = 0$) has components in two of the basis states: $m_J = \frac{3}{2}$ and $-\frac{1}{2}$, or $m_J = -\frac{3}{2}$ and $+\frac{1}{2}$. A $\Delta n = 2$ transition proceeds via an intermediate state in the conduction band, and the matrix element is

$$\sim (u_{3/2,1/2} | p_+ | iS)(iS | p_+ | u_{3/2,-3/2}).$$

To lowest order in H and at $k_x = 0$, the matrix elements for various transitions involving light and heavy holes are given by

$$A_{f0} = N_{f0} \frac{P^2}{mE_G} \frac{E_G^2}{E_G^2 - (\hbar \omega_0)^2} \left(\frac{\epsilon_{0x} + i\epsilon_{0y}}{\sqrt{2}} \right) \left(\frac{\epsilon_{1x} - i\epsilon_{1y}}{\sqrt{2}} \right), \quad (4)$$

where the numerical factors N_{f0} are listed in Table II. The heavy hole to light hole transitions are best suited to experimental work (since in very large fields there may be no light holes at low temperatures) and they also have the largest Raman shifts. The calculation was extended to the next order (i.e., $\hbar \omega_c/E_G$) for these transitions, and the results are plotted on Fig. 2 for InSb. (The corrections are negligible in InP.) It is perhaps surprising that although at 30 kG the ratio $\hbar \omega_c/E_G$ is only 0.1 the correction to A_{f0} is as large as it is, e.g., for the $|hh,1\uparrow\rangle$ to $|lh,3\uparrow\rangle$ transition. The apparent reason is that the terms first order in H have large numerical coefficients of the order of 2 to 10. For quantitative estimates of the valence band A_{f0} at these high fields one should make an "exact" (in H) calculation using the states of Table I.

From Figs. 2 and 3 we see that the matrix elements for Raman scattering in the valence band are comparable (unlike in the conduction band) for InSb and InP, and this is because A_{f_0} in the valence band is inversely proportional to only the first power of E_G .

(b) *Spin Reversal Transitions*

Somewhat arbitrarily, we denote by spin-reversal transitions in the valence band, those processes which involve one photon polarized parallel to H and one polarized transverse to H . This terminology agrees with that in the conduction band. Because of the opposite curvatures of the conduction and valence bands the transitions between holes have polarizations opposite to those of the transitions with the same Δn in the conduction band. The matrix elements are of order P^2/mE_G and can readily be obtained if needed.

III. CONCLUSION

The cross sections calculated above are sufficiently large to permit the observation of the Raman transi-

tions with a laser source. Thus for the $|hh,0\rangle$ to $|lh,1\rangle$ transition in InP, a differential cross-section of $(d\sigma/d\Omega) \sim 2 \times 10^{-23}$ cm² is given on Fig. 3. This can be compared with an observed⁵ total cross-section of $\sigma \sim 5 \times 10^{-24}$ cm² for F centers in alkali halides. An advantage of Raman spectroscopy is the large value of $\omega_c\tau$ which can be reached with a high magnetic field. For example the mobility⁶ at 77°K of p -type InP with 10^{16} impurities per cc corresponds to $\omega_c\tau \sim 7$ for the light holes at 100 kG. Thus for large (and of course, small) band gap materials the Raman transitions in the valence band as well as the spin-reversal transitions can be of use in band structure measurements.

ACKNOWLEDGMENT

The author is grateful to P. A. Wolff for suggesting some of these calculations and for several informative discussions.

⁵ J. M. Worlock and S. P. S. Porto, Phys. Rev. Letters **15**, 697 (1965); C. H. Henry, (to be published).

⁶ M. Glicksman and K. Weiser, J. Phys. Chem. Solids **10**, 337 (1959).

Erratum

Nuclear Quadrupole Resonance by Nuclear Induction: Theory and Experiment; with an Extension of the Theory to Absorption Methods, GEORGE W. SMITH [Phys. Rev. **149**, 346 (1966)]. C. Dean [Phys. Rev. **96**, 1053 (1954)] first predicted the applicability of the Bloch crossed-coil apparatus to NQR experiments.